

Role of Aromatic Side Chains in the Folding and Thermodynamic Stability of Integral Membrane Proteins

Heedeok Hong, Sangho Park, Ricardo H. Flores Jiménez, Dennis Rinehart, and Lukas K. Tamm*

Contribution from the Department of Molecular Physiology and Biological Physics, University of Virginia Health System, P.O. Box 800736, Charlottesville, Virginia 22908-0736

Received December 11, 2006; E-mail: lkt2e@virginia.edu

Abstract: Aromatic residues are frequently found in helical and β -barrel integral membrane proteins enriched at the membrane–water interface. Although the importance of these residues in membrane protein folding has been rationalized by thermodynamic partition measurements using peptide model systems, their contribution to the stability of bona fide membrane proteins has never been demonstrated. Here, we have investigated the contribution of interfacial aromatic residues to the thermodynamic stability of the β -barrel outer membrane protein OmpA from *Escherichia coli* in lipid bilayers by performing extensive mutagenesis and equilibrium folding experiments. Isolated interfacial tryptophanes contribute -2.0 kcal/mol, isolated interfacial tyrosines contribute -2.6 kcal/mol, and isolated interfacial phenylalanines contribute -1.0 kcal/mol to the stability of this protein. These values agree well with the prediction from the Wimley–White interfacial hydrophobicity scale, except for tyrosine residues, which contribute more than has been expected from the peptide models. Double mutant cycle analysis reveals that interactions between aromatic side chains become significant when their centroids are separated by less than 6 Å but are nearly insignificant above 7 Å. Aromatic–aromatic side chain interactions are on the order of -1.0 to -1.4 kcal/mol and do not appear to depend on the type of aromatic residue. These results suggest that the clustering of aromatic side chains at membrane interfaces provides an additional heretofore not yet recognized driving force for the folding and stability of integral membrane proteins.

Introduction

Aromatic side chains such as Trp, Tyr, and Phe are known to play a unique role in the folding and assembly of integral membrane proteins.¹ Statistical analysis of membrane proteins of known structure^{2–8} and genomic database searches^{8–10} for identifying transmembrane segments of α -helical and β -barrel membrane proteins show that aromatic residues are significantly enriched at the membrane–water interface. Physicochemical studies using peptide model systems indicate that these residues also have a high tendency to partition into the membrane–water interface.¹¹ These residues in fact exceed all other residues in their ability to partition into the interface region of membranes and, therefore, are the most highly ranked on the experimentally

derived thermodynamic Wimely–White (WW) interface hydrophobicity scale.^{11,12} The major driving force for the preferred interfacial localization is thought to be the hydrophobic effect, but dipole–dipole and hydrogen-bonding interactions in the interface region of the lipid bilayer also contribute.^{12–14} More recent work using a biological read-out of nascent polypeptide chain incorporation into membranes confirms the model peptide studies in two important ways: the bulky aromatic residues Trp and Tyr stabilize polypeptide insertion when placed in the interfacial region but put a penalty on insertion when placed in the central region of the bilayer.¹⁵ These results strongly suggest that the aromatic side chains play an important role in correctly anchoring and positioning integral membrane proteins in the lipid bilayer of biological and model membranes.

Despite these highly suggestive results from the model polypeptide studies in vitro and in vivo, it is of considerable interest to know whether the previously obtained partition energies are directly applicable to understanding the roles of aromatic side chains in the folding and stability of integral membrane proteins with defined three-dimensional structures. Differences could potentially arise because the model peptides

- (1) Killian, J. A.; von Heijne, G. *Trends Biochem. Sci.* **2000**, *25*, 429–34.
- (2) Wallin, E.; Tsukihara, T.; Yoshikawa, S.; von Heijne, G.; Elofsson, A. *Protein Sci.* **1997**, *6*, 808–15.
- (3) Ulmschneider, M. B.; Sansom, M. S. *Biochim. Biophys. Acta* **2001**, *1512*, 1–14.
- (4) Granseth, E.; von Heijne, G.; Elofsson, A. *J. Mol. Biol.* **2005**, *346*, 377–85.
- (5) Ulmschneider, M. B.; Sansom, M. S.; Di Nola, A. *Proteins* **2005**, *59*, 252–65.
- (6) Adamian, L.; Nanda, V.; DeGrado, W. F.; Liang, J. *Proteins* **2005**, *59*, 496–509.
- (7) Senes, A.; Chadi, D. C.; Law, P. B.; Walters, R. F.; Nanda, V.; DeGrado, W. F. *J. Mol. Biol.* **2007**, *366*, 436–48.
- (8) Wimley, W. C. *Protein Sci.* **2002**, *11*, 301–12.
- (9) Landolt-Marticorena, C.; Williams, K. A.; Deber, C. M.; Reithmeier, R. A. *J. Mol. Biol.* **1993**, *229*, 602–8.
- (10) Wallin, E.; von Heijne, G. *Protein Sci.* **1998**, *7*, 1029–38.
- (11) Wimley, W. C.; White, S. H. *Nat. Struct. Biol.* **1996**, *3*, 842–8.

- (12) Wimley, W. C.; Creamer, T. P.; White, S. H. *Biochemistry* **1996**, *35*, 5109–24.
- (13) Wimley, W. C.; White, S. H. *Biochemistry* **1993**, *32*, 6307–12.
- (14) Yau, W. M.; Wimley, W. C.; Gawrisch, K.; White, S. H. *Biochemistry* **1998**, *37*, 14713–8.
- (15) Hessa, T.; Kim, H.; Bihlmaier, K.; Lundin, C.; Boekel, J.; Andersson, H.; Nilsson, I.; White, S. H.; von Heijne, G. *Nature* **2005**, *433*, 377–81.

are designed to partition into membrane interfaces and the segments of the model membrane proteins that are inserted across the membrane may have variable backbone topologies relative to the lipid bilayer. The backbones of the polypeptides used in these model systems may be much more pliable and may adapt to particular experimental situations to optimize partitioning than would be expected for bona fide membrane proteins with defined three-dimensional structures. This difference may impose different conformational restrictions on aromatic side chains in different systems, which may affect the partition and folding energies. In addition, testing the role of aromatic side chains in the folding and stability of a multipass integral membrane protein with a defined structural frame provides new opportunities to examine the influence of structural contexts; for example, the effect of nearest neighbor interactions on membrane protein stability and folding may be studied. New opportunities may include studies of the influence of the secondary structure of the backbone and the depth of the residue within the lipid bilayer¹⁵ as well as hydrogen-bonding,^{16,17} π -cation,¹⁸ and aromatic stacking interactions.¹⁹

We have recently developed a reversible folding system of an integral membrane protein in lipid bilayers using the *E. coli* outer membrane protein A (OmpA) as a model.²⁰ OmpA is a monomeric 35 kDa protein composed of an N-terminal transmembrane (TM) and a C-terminal periplasmic domain.²¹ The TM domain, the structure of which has been solved by X-ray crystallography²² and solution NMR spectroscopy,²³ folds into an 8-stranded β -barrel and forms a small gated pore in model and biological membranes.^{24–26} Equilibrium folding studies with OmpA in lipid bilayers have enabled us to elucidate several effects of the physical properties of the lipid bilayer on the stability of this membrane protein.²⁰ The system has also allowed us to measure the strengths of salt-bridge interactions and thus to propose a new mechanism for the gating of the OmpA channel.²⁶ Since the fully denatured state of OmpA is completely dissociated from the lipid bilayer,²⁰ it is possible to rigorously assess the contribution of the folding of specific amino acid residues, which includes their partitioning from the aqueous into the membrane phase, to the stability of this membrane protein. The outer surface of the OmpA TM domain that contacts the lipid bilayer shows features that are typical for most α -helical bundle and all β -barrel membrane proteins:²² it consists of a nonpolar belt with the amino acid composition $L_8V_4A_4T_3G_3I_2M_1$ in the central region of lipid bilayer and two bands that are highly enriched in aromatic residues with amino acid compositions $W_3Y_2F_1$ and $W_1Y_5F_2$ near the outer surface and periplasmic interface of the outer membrane, respectively. In this study, we

have measured the contribution of many of these aromatic residues to the thermodynamic stability of OmpA. Among the 14 aromatic residues contacting the lipid bilayer interface, we individually mutated four Trp, five Tyr, and three Phe residues to Ala and compared the thermodynamic stability of the mutant proteins to that of the wild-type protein. Ala was chosen as a reference amino acid residue because it has an intermediate hydrophobicity^{11,12} and its statistical distribution in integral membrane proteins has little positional dependence across the lipid bilayer.^{3,8} We also employed double mutant cycle analysis^{26,27} to estimate the strengths of interactions between two neighboring aromatic side chains. Our results suggest that interfacial aromatic side chains contribute significantly, individually and even more when clustered, to the thermodynamic stability of integral membrane proteins.

Methods

Site-Directed Mutagenesis and Purification of OmpA. Site-directed mutagenesis was carried out using the QuickChange kit (Stratagen) and the plasmid pET1113²⁸ as a template. The vector containing the wild-type or mutated proOmpA gene with signal sequence was transformed into BL21(DE3) [$\Delta lamB ompF::Tn5 \Delta ompA \Delta ompC$].²⁹ The procedure described here essentially follows that of Surrey and Jähnig with some modifications.³⁰ The transformed *E. coli* BL21(DE3) [$\Delta lamB ompF::Tn5 \Delta ompA \Delta ompC$] cells were grown in LB-media at 37 °C. An amount of 0.5 mL of 1 M IPTG was added to 1 L culture approximately when it reached an optical density (OD) value of 0.6. The cells were grown for about 4 to 5 h after induction. The wet cell paste was resuspended in solution A [15 mL per 1 L culture; 0.75 M sucrose, 10 mM TrisHCl, pH 5, and 0.05% β -mercaptoethanol (v/v)] using an ice/water cooling bath. Solution B (10 mL per 1 L culture; 40 mM EDTA, 0.05% β -mercaptoethanol, 10 mM TrisHCl, pH 7.1) was then added while the mixture was stirred and ice cooled. Lysozyme was added to a concentration of 50 μ g/mL, and the mixture was stirred for 1 h at room temperature. The β -mercaptoethanol concentration was increased to 0.2% total. The solution was French-pressed two times. The cell lysate was brought slowly to a final concentration of 6 M urea (Sigma, SigmaUltra grade) under stirring with small amounts of solid urea sequentially added. Titanium dust and remaining nondigested cells were removed by centrifugation at 2000 g (5 °C, 30 min). The solution was centrifuged at 32 000 rpm (4 °C, for a minimum of 6 h). The precipitate contained the pre-extracted membrane fraction.

Each of 40 mL and 0.5 L of 8 M urea solutions (40 mL: Sigma, SigmaUltra grade; 0.5 L: Sigma, ACS reagent grade 99.0~100.5%) per 1 L *E. coli* culture were purified by passing over a cation/anion exchange column (mixed bead, Biorad AG 501-X8) to remove isocyanate contamination of urea. Isocyanate reacts with SH or NH₂ groups of proteins and should therefore be avoided as much as possible. The pre-extracted membranes were resuspended in 10 mL (per 1 L culture) of the freshly purified 8 M SigmaUltra grade urea solution, containing 20 mM TrisHCl, pH 8.0, and 0.1% β -mercaptoethanol by the use of a Potter homogenizer at room temperature. A nominal 10 mL of isopropanol were added to give a total volume of ~20 mL. A white precipitate formed at this time. The whole mixture in a glass vial was then incubated at the temperature range of 54~55 °C in a preheated water bath for exactly 30 min to extract OmpA. This step is critical as urea develops significant amounts of isocyanate when warmed

(16) Meindl-Beinker, N. M.; Lundin, C.; Nilsson, I.; White, S. H.; von Heijne, G. *EMBO Rep.* **2006**, *7*, 1111–6.

(17) Zhou, F. X.; Cocco, M. J.; Russ, W. P.; Brunger, A. T.; Engelman, D. M. *Nat. Struct. Biol.* **2000**, *7*, 154–60.

(18) Gallivan, J. P.; Dougherty, D. A. *Proc. Natl. Acad. Sci. U.S.A.* **1999**, *96*, 9459–64.

(19) Burley, S. K.; Petsko, G. A. *Science* **1985**, *229*, 23–8.

(20) Hong, H.; Tamm, L. K. *Proc. Natl. Acad. Sci. U.S.A.* **2004**, *101*, 4065–70.

(21) Schweizer, M.; Hindennach, I.; Garten, W.; Henning, U. *Eur. J. Biochem.* **1978**, *82*, 211–7.

(22) Pautsch, A.; Schulz, G. E. *Nat. Struct. Biol.* **1998**, *5*, 1013–7.

(23) Arora, A.; Abildgaard, F.; Bushweller, J. H.; Tamm, L. K. *Nat. Struct. Biol.* **2001**, *8*, 334–8.

(24) Arora, A.; Rinehart, D.; Szabo, G.; Tamm, L. K. *J. Biol. Chem.* **2000**, *275*, 1594–600.

(25) Bond, P. J.; Faraldo-Gomez, J. D.; Sansom, M. S. *Biophys. J.* **2002**, *83*, 763–75.

(26) Hong, H.; Szabo, G.; Tamm, L. K. *Nat. Chem. Biol.* **2006**, *2*, 627–35.

(27) Horovitz, A.; Serrano, L.; Avron, B.; Bycroft, M.; Fersht, A. R. *J. Mol. Biol.* **1990**, *216*, 1031–44.

(28) Kleinschmidt, J. H.; den Blaauwen, T.; Driessen, A. J.; Tamm, L. K. *Biochemistry* **1999**, *38*, 5006–16.

(29) Prilipov, A.; Phale, P. S.; Van Gelder, P.; Rosenbusch, J. P.; Koebnik, R. *FEMS Microbiol. Lett.* **1998**, *163*, 65–72.

(30) Surrey, T.; Jähnig, F. *Proc. Natl. Acad. Sci. U.S.A.* **1992**, *89*, 7457–61.

up. After the extraction was finished, the sample was rapidly cooled by putting it into ice until it reached a temperature below 10 °C. The mixture was then centrifuged at 28 000 rpm at 4 °C for at least 90 min. The clear supernatant containing unfolded OmpA was taken and further purified by ion exchange chromatography (25 mL Q Sepharose column, fast flow, Pharmacia) at room temperature. Three buffers were prepared (equilibration buffer: 50 mL isopropanol mixed with 50 mL of the buffer solution containing 15 mM TrisHCl, pH 8.5, 0.1% β -mercaptoethanol, and 8 M reagent grade urea. Wash-buffer: 500 mL, 15 mM TrisHCl, pH 8.5, 0.05% β -mercaptoethanol, and 8 M urea. Elution-buffer: 200 mL, 15 mM TrisHCl, pH 8.5, 0.05% β -mercaptoethanol, 8 M urea, and 100 mM NaCl). The solutions were sterile-filtered and degassed prior to their use on the FPLC. The column was equilibrated using the 50% isopropanol containing equilibration buffer (1 mL/min flow). The solution containing OmpA was loaded onto the column, and the column was washed using the wash buffer. The salt content of the buffer in the column was then gradually increased using the second FPLC input line with wash and elution buffers. The combined OmpA fractions identified by SDS-PAGE were concentrated by ultrafiltration to a final concentration of 20 to 50 mg/mL as estimated by the Bradford protein assay. The whole procedure took 5 days from the large scale culture of *E. coli* cells to the final concentration of proteins, and longer preparation times were avoided. The concentrated proteins were stored at -20 °C and used for the stability measurements within 1 month after the purification.

Urea-Induced Equilibrium Unfolding and Refolding. Concentrated OmpA unfolded in 8 M urea was diluted 50–100 fold in 10 mM SUVs to a final protein concentration of 12 μ M. The refolding was incubated for 3 h at 37 °C. The refolded OmpA-lipid complex was further diluted in aliquots of different urea concentrations in 10 mM glycine buffer (1 mM EDTA, pH, 9.2). The dilution was 10 fold for fluorescence and 2.5 fold for SDS-PAGE experiments. The equilibrium refolding for SDS-PAGE was done by adding the unfolded OmpA stock into aliquots of 4 mM SUV solutions at appropriate urea concentrations to yield a final protein concentration of 4.8 μ M. The unfolding and refolding reactions were incubated at 37 °C overnight to reach equilibrium.

Steady-State Fluorescence Spectroscopy. Fluorescence spectra were collected in a Fluorolog-3 spectrofluorometer (Jobin-Yvon, Edison, N.J.). The excitation wavelength was 290 nm and Trp fluorescence of OmpA was measured over 300 to 400 nm range at a scan rate of 0.15 nm/sec. The 4.2 nm slits were used for both excitation and emission. All spectra were background-corrected with a proper reference sample of identical composition but without protein.

Small Unilamellar Vesicles. Stock solutions of 1,2-dipalmitoleoyl-*sn*-glycero-3-phosphocholine (diC_{16:1}PC) and 1-palmitoyl-2-oleoyl-*sn*-glycero-3-[phospho-*rac*-(1-glycerol)] (C_{16:0}C_{18:1}PG) from Avanti Polar Lipids dissolved in chloroform were mixed in a glass test tube at a molar ratio of 9:1 (diC_{16:1}PC:C_{16:0}C_{18:1}PG). A total of 12 μ mol of lipid was dried under a stream of nitrogen and further in a high-vacuum desiccator overnight. The dried lipid was thoroughly mixed with 1.2 mL of glycine buffer to yield a final lipid concentration of 10 mM. The lipid dispersion was sonicated for 50 min in an ice–water bath using a Branson ultrasonifier microtip at 50% duty cycle. After removal of titanium dust by centrifugation at 8000 rpm for 15 min twice, the resulting SUVs were equilibrated overnight at 4 °C.

SDS-PAGE Shift Assay. The equilibrated samples were mixed with the same volume of treatment buffer. The mixtures were loaded on 12.5% SDS-PAGE without boiling.

Fitting of Equilibrium Unfolding Curves to Two-State Model. The procedure described here is essentially the same as the procedure previously described in Hong and Tamm.²⁰ Fluorescence spectra were parameterized by calculating an average emission wavelength, $\langle\lambda\rangle$, defined as $\langle\lambda\rangle = \frac{\sum(F_i\lambda_i)}{\sum(F_i)}$. λ_i and F_i are the wavelength and the corresponding fluorescence intensity at the *i*th measuring step in the spectrum. The unfolding curves, $\langle\lambda\rangle$ versus [urea], were fitted to the following form of the two-state model

$$\langle\lambda\rangle = \frac{\langle\lambda\rangle_F + \langle\lambda\rangle_U \frac{1}{Q_R} \exp[m([\text{denaturant}] - C_m)/RT]}{1 + \frac{1}{Q_R} \exp[m([\text{denaturant}] - C_m)/RT]} \quad (1)$$

using Wavemetrics IgorPro software. $\langle\lambda\rangle_F$ and $\langle\lambda\rangle_U$ are the average emission wavelengths of the folded and unfolded states, respectively, determined from linear extrapolations to 0 M urea of the plateau values of the two states. C_m is the urea concentration where the fractions of folded and unfolded states are equal. Q_R is the relative ratio of the total fluorescence intensity of the native state to that of the unfolded state and is needed for normalization when one uses $\langle\lambda\rangle$ values to represent species concentrations. The free energy of unfolding is obtained from the fitted values of C_m and m :

$$\Delta G^\circ_{u,H_2O} = mC_m \quad (2)$$

Results

Distribution of Aromatic Side Chains on the Surface of OmpA. Figure 1 shows the preferred disposition of the aromatic side chains near the top and bottom of the β -barrel of OmpA where the protein contacts the outer and periplasmic interfacial regions of the lipid bilayer.³¹ Except for Phe51, whose side-chain centroid is located approximately 4.5 Å below the center of the bilayer, all other aromatic residues are located approximately between 7 and 12 Å from the center of the bilayer. Even within these two aromatic belts, these residues are not uniformly distributed. Four aromatic residues are isolated (> 10 Å) from aromatic nearest neighbors. These are Trp15 (strand β 1) on the outer belt and Tyr129 (strand β 6), Tyr48 (turn T1), and Tyr85 (strand β 4) on the inner periplasmic belt. The centroid of the indole ring of Trp15 is separated from the centroid of the phenyl ring of Tyr141 by 10.4 Å. Similarly, Tyr129 is separated from its nearest neighboring aromatic residue Tyr85 by 14.2 Å. Besides these isolated residues, there are three regions, in which two or three aromatic residues are clustered within 6 Å of each other. In the outer belt, Trp143 (strand β 7) is sandwiched between Phe123 (strand β 6) and Tyr141 (strand β 7) with interaromatic distances of 5.5 and 5.8 Å, respectively. In the inner periplasmic belt, Trp7 (strand β 1) is located 4.8 Å from Tyr43 (strand β 2) and Tyr168 (strand β 8) is within 5.1 Å from Phe170 (strand β 8). Other aromatic pairs are located at intermediate distances (6 to 10 Å) from each other: Tyr55 and Tyr57 in the outer belt are 7.4 Å apart, Tyr43 and Phe51 in the inner periplasmic belt are 7.7 Å apart, and Trp7 and Tyr168 in the inner periplasmic belt are 8.3 Å apart from each other.

Effects of Single Aromatic to Ala Mutations on the Stability of OmpA. As a first step to obtain quantitative information on the contribution of aromatic residues on the stability of OmpA in lipid bilayers, we individually mutated four Trp, five Tyr, and three Phe residues to Ala and measured the thermodynamic stability of each mutant. A bilayer system consisting of diC_{16:1}PC and C_{16:0}C_{18:1}PG (9:1) was chosen because the hydrophobic thickness of diC_{16:1}PC (23.5 Å)³² matches the hydrophobic thickness of the outer membranes of Gram-negative bacteria (23.7 ± 1.3 Å).³³ The effect of bilayer thickness on the stability of OmpA has been studied previously.²⁰ Although the major phospholipid class in *E. coli* is

(31) Pautsch, A.; Schulz, G. E. *J. Mol. Biol.* **2000**, *298*, 273–82.

(32) Lewis, B.; Engelman, D. M. *J. Mol. Biol.* **1983**, *166*, 211–217.

(33) Lomize, A. L.; Pogozheva, I. D.; Lomize, M. A.; Mosberg, H. I. *Protein Sci.* **2006**, *15*, 1318–33.

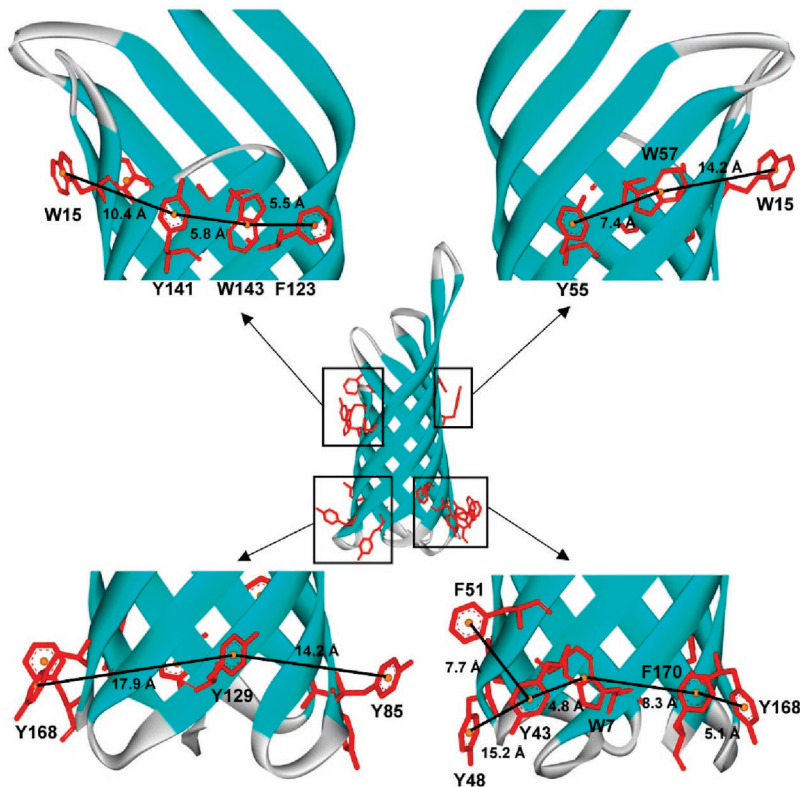


Figure 1. Structure of transmembrane domain of OmpA showing the spatial arrangements of aromatic side chains that contact the membrane in the outer leaflet interface (top) and periplasmic leaflet interface (bottom). The distances between the centroids of the aromatic rings are indicated with lines. The figure was prepared with the program Weblab Viewer using the PDB file 1QJP.³¹

phosphatidylethanolamine, we chose phosphatidylcholine as our reference lipid because it is the standard lipid in eukaryotic membranes and therefore has been chosen in almost all folding studies of membrane proteins. We know that phosphatidylethanolamines increase the absolute free energies of insertion of OmpA,³⁴ but all data reported here are difference free energies (aromatic minus alanine, or aromatic–aromatic interactions from double mutant cycles), which we expect not to be affected much by the choice of lipid headgroup or bilayer thickness.

Figure 2 shows representative urea-induced equilibrium unfolding curves of the three groups of aromatic mutant proteins in lipid bilayers measured by Trp fluorescence. These data were fitted to the two-state folding model according to eq 1 (Methods). Our previous studies showed that this treatment is justified because the curves are fully reversible and can also be reproduced by other methods that report on different kinetic phases of OmpA folding such as far-UV CD spectroscopy or an SDS-PAGE shift assay.^{20,34}

The fitted parameters for wild-type and the mutant proteins and the calculated the free energies of unfolding ($\Delta G_{u,H_2O}^\circ$) are listed in Table 1. The contributions to the stability of each mutation relative to that of wild-type [$\Delta\Delta G_u^\circ = \Delta G_{u,H_2O}^\circ$ (wild-type) – $\Delta G_{u,H_2O}^\circ$ (mutant)] are shown in the second to last column of Table 1.

A first cursory inspection of these data does not reveal a clear pattern of common stabilizing energies that could be assigned to each type of residue. Moreover, the contribution of these residues to the stability of OmpA in membranes does not

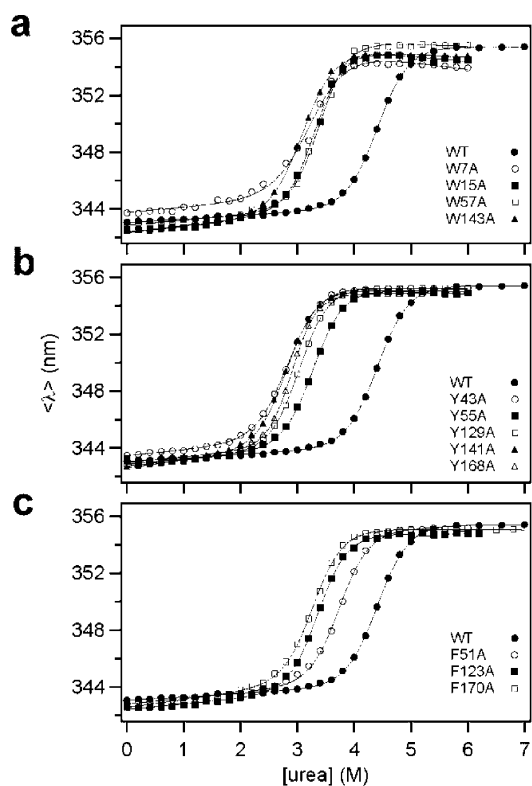


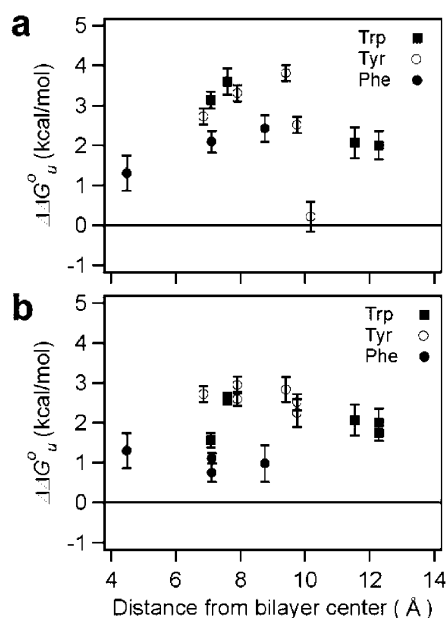
Figure 2. Equilibrium unfolding of wild-type and mutant OmpAs with individual aromatic residues substituted with alanines: (a) Trp → Ala substitutions, (b) Tyr → Ala substitutions, and (c) Phe → Ala substitutions.

correlate with the distances of these residues from the membrane center (Figure 3a).

(34) Tamm, L. K.; Hong, H.; Liang, B. *Biochim. Biophys. Acta* **2004**, *1666*, 250–63.

Table 1. Thermodynamic Parameters of Urea-Induced Unfolding of Wild-Type and Mutant OmpAs in Lipid Bilayers

	C_m M	m kcal/mol M ⁻¹	$\Delta G_{u,H_2O}^o$ kcal/mol	$\Delta\Delta G_u^o$ kcal/mol	Classification of mutated residues
wild-type	4.2	2.2 ± 0.1	9.3 ± 0.2	0	
W7A	3.0	1.9 ± 0.1	5.7 ± 0.3	3.6	clustered
W15A	3.1	2.4 ± 0.1	7.3 ± 0.4	2.0	isolated
W57A	3.1	2.4 ± 0.1	7.3 ± 0.3	2.0	intermediate
W143A	2.8	2.2 ± 0.1	6.2 ± 0.1	3.1	clustered
Y43A	2.6	2.2 ± 0.1	5.5 ± 0.1	3.8	clustered
Y55A	3.1	2.2 ± 0.1	6.8 ± 0.1	2.5	intermediate
Y129A	2.8	2.4 ± 0.1	6.6 ± 0.1	2.7	isolated
Y141A	2.6	2.3 ± 0.1	6.0 ± 0.1	3.3	clustered
Y168A	2.9	3.1 ± 0.1	9.1 ± 0.2	0.2	clustered
F51A	3.5	2.3 ± 0.1	8.1 ± 0.3	1.2	isolated
F123A	3.1	2.3 ± 0.1	7.2 ± 0.2	2.1	clustered
F170A	3.0	2.3 ± 0.1	6.9 ± 0.3	2.4	clustered
W7A/Y43A	1.6	1.9 ± 0.1	2.9 ± 0.1	6.4	
Y55A/W57A	2.1	2.4 ± 0.1	5.1 ± 0.1	4.2	
Y168A/F170A	2.6	3.1 ± 0.1	8.1 ± 0.3	1.2	
F123A/W143A	2.4	2.3 ± 0.1	5.4 ± 0.2	4.9	
F123A/Y141A	1.9	2.1 ± 0.1	4.0 ± 0.2	5.3	
Y141A/W143A	1.6	2.2 ± 0.1	3.6 ± 0.1	5.7	
F123A/Y141A/W143A	1.2	2.0 ± 0.1	2.5 ± 0.1	6.8	

**Figure 3.** Dependence of contribution of aromatic side chains to the free energies of unfolding of OmpA on their distance from the bilayer center in the native structure: (a) raw data (column 5 of Table 1); (b) data corrected for aromatic–aromatic nearest neighbor interactions (column 4 of Table 3).

However, taking into consideration the nearest aromatic neighbors reveals some interesting trends. Trp7 and Trp143 stabilize OmpA by -3.6 kcal/mol and -3.1 kcal/mol, respectively, and thus have the strongest stabilizing effect of the four tryptophanes on the protein. Trp7 is within 4.8 Å from Tyr43 and Trp143 is sandwiched between Phe123 and Tyr141 (Table 2). Trp15 and Trp57 are more isolated and stabilize OmpA by only -2.0 kcal/mol each. Since “isolated” aromatic residues have nonaromatic nearest neighbors, we checked whether any of these could potentially contribute nonaromatic neighboring interactions. Trp15 has Leu13, Gln17, Asn33, Leu35, Ala37, Gly160, Leu162, and Leu164 within a radius of 10 Å (C_α positions) and the nearest neighbors of Trp57 are Ala37, Ala39,

Table 2. Distances and Interaction Energies of Pairs of Aromatic Side Chains of OmpA

aromatic interaction	distance between centroids of aromatic residues (Å)	interaction energy $\Delta\Delta G_{\text{inter}}^o$, kcal/mol ^a
Trp7–Tyr43	4.8	-1.0
Tyr168–Phe170	5.1	-1.4
Phe123–Trp143	5.5	-1.3
Tyr141–Trp143	5.8	-0.7
Tyr55–Trp57	7.4	-0.3
Phe123–Tyr141	11.0	-0.1
Trp7–Phe170	8.3	n.d.
Trp43–Phe51	7.7	n.d.

^a n.d. = not determined.

Gly41, Met53, Tyr55, Gln75, Val77, and Leu79. Except for Asn33, which is H-bonded to Trp15, none of these residues have the potential for interactions with the indole rings. Specifically, there are no sites for potential π -cation interactions that are relatively frequent in soluble proteins.¹⁸ The interactions of the other two tryptophanes also seem to be restricted to aromatic stacking interactions because the other neighboring residues of Trp7 are Asn5, Thr9, Gly41, and Val45, and those of Trp143 are Pro121, Gly125, Asn145, Gly160, and Leu162. The H-bond interactions are not significant (there are also some between Gln75 and Tyr55 and between Asn5 and Tyr43) as will become evident from the analysis below. The reason for this indifference to aromatic H-bonds is probably that these residues are all located in the membrane interface and therefore may form alternative H-bonds to water with negligible energy differences.

Similar trends are observed with interfacial tyrosines and phenylalanines. Tyr43 and Tyr141 have the strongest stabilizing effects on the folding of OmpA. Their contributions to the protein’s stability are -3.8 and -3.3 kcal/mol, respectively. Both residues have neighboring aromatic residues within a radius of less than 6 Å (Figure 1). Tyr43 and Trp7 are only 4.8 Å and Tyr141 and Trp143 are only 5.8 Å apart from each other (Table 2). By contrast, the stabilizing effect of Tyr55 and Tyr129, which are more isolated from neighboring aromatic residues, are -2.5

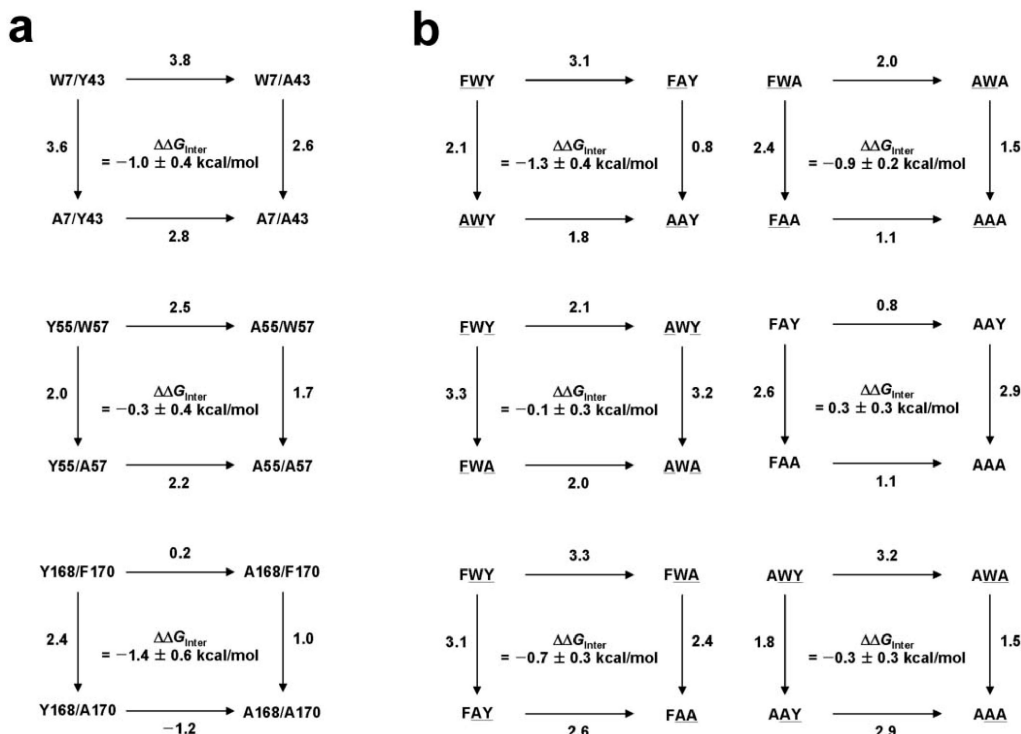


Figure 4. Mutant cycles for estimating interaction energies between pairs of aromatic side chains: (a) double mutant cycles probing the interactions between Trp7 and Tyr43, Tyr55 and Trp57, and Tyr168 and Phe170; (b) double mutant cycles used to construct a triple mutant cycle for the complete thermodynamic analysis of the pairwise interactions within the aromatic triad consisting of Phe123, Tyr141, and Trp143. The three capital letter codes stand for the three residues in positions 123, 143, and 141, respectively, of wild-type and mutant OmpAs. The pairs of residues whose interaction energies are determined in each cycle are underlined.

and -2.7 kcal/mol, respectively. Phe123 and Phe170 are more stabilizing than Phe51 ($\Delta\Delta G^\circ = -2.1$, -2.4 , and -1.2 kcal/mol, respectively). Phe123 is close to Trp143 and Phe170 is close to Tyr168, whereas Phe51 is more isolated (Figure 1, Table 2). The phenyl ring of Phe51 is also located deeper in the membrane, which may explain its comparatively smaller stabilization energy. An interesting case is Tyr168, which contributes only -0.2 kcal/mol to the stability of OmpA. This unusually small energy can be traced to the exceptionally large m -value of 3.1 kcal/mol M^{-1} . The m -values of most other mutants of this study are of the order of 2.2 kcal/mol M^{-1} (Table 1). Although the midpoint of transition of the Y168A mutant is shifted to 2.9 from 4.2 M of wild-type, the larger m -value results in a higher $\Delta G^\circ_{\text{u,H}_2\text{O}}$. This larger m -value of Y168A (and also of double mutant Y168A/F170A, see below) is not due to experimental errors, but is statistically significant as reproduced in repeated measurements using different preparations. Variations in m -values in solvent-induced protein denaturation experiments are often attributed to changes in exposed surface areas upon unfolding, which may be interpreted as differences in denatured state ensembles of two proteins.³⁵ Tyr168 and Phe170 are also close in sequence to each other and their mutation may, therefore, perturb the denatured state ensembles that are typically observed for wild-type and the other mutants, which precludes a direct comparison of the folding energies of Y168A (and Y168A/F170A) with those of the other proteins.

Pairwise Interaction Energies between the Closely Spaced Aromatic Residues. It is evident from the results obtained with single mutants that the close proximity of aromatic residues

further stabilizes OmpA. To better estimate the strengths of aromatic side-chain interactions, we analyzed them further by double mutant cycle analysis. The strategy is to mutate each of the interacting residues (X and Y) of protein P into noninteracting side chains (e.g., alanines) in single and double mutants and to measure the free energies of unfolding, $\Delta G^\circ_{\text{u,H}_2\text{O}}$, of wild-type (P-XY), both single mutants (P-X and P-Y), and the double mutant (P). The interaction energy, $\Delta\Delta G_{\text{inter}}$, between X and Y is then determined from a thermodynamic cycle that is constructed from the free energies of unfolding of all four species:³⁶

$$\Delta\Delta G_{\text{inter}} = -[\Delta G^\circ_{\text{u,H}_2\text{O}}(\text{P-XY}) - \Delta G^\circ_{\text{u,H}_2\text{O}}(\text{P-X})] + [\Delta G^\circ_{\text{u,H}_2\text{O}}(\text{P-Y}) - \Delta G^\circ_{\text{u,H}_2\text{O}}(\text{P})] \quad (3)$$

which under the assumption that the two residues of interest are not interacting in the unfolded state is equivalent to

$$\Delta\Delta G_{\text{inter}} = -[\Delta G_{\text{P-XY} \rightarrow \text{P-X}} - \Delta G_{\text{P-Y} \rightarrow \text{P}}] \quad (4)$$

where $\Delta G_{\text{P-XY} \rightarrow \text{P-X}}$ is the free energy difference between the folded states of wild-type and mutant P-X and $\Delta G_{\text{P-Y} \rightarrow \text{P}}$ is the free energy difference between the folded states of mutant P-Y and double mutant P.

We performed double mutant cycle analysis on two aromatic pairs, Trp7-Tyr43 and Tyr168-Phe170, with distances of less than 6 \AA (4.8 and 5.1 \AA , respectively) and one pair, Tyr55-Trp57, with a distance of 7.4 \AA . The results of these experiments are shown in Figure 4a. Double mutant cycles performed to

(35) Wrabl, J.; Shortle, D. *Nat. Struct. Biol.* **1999**, *6*, 876-83.

(36) Fersht, A. R.; Matouschek, A.; Serrano, L. *J. Mol. Biol.* **1992**, *224*, 771-82.

probe interactions in the aromatic triad consisting of residues Phe123, Trp143, and Tyr141 are shown in Figure 4b.

The individual free energies of unfolding, $\Delta G_{u,H_2O}^0$, of the mutants are listed in Table 1, and the resulting interaction energies between pairs of aromatic side chains along with their separation distances are shown in Table 2. The relatively closely spaced aromatic pairs Trp7–Tyr43, Tyr168–Phe170, Phe123–Trp143, and Tyr141–Trp143 all interact with interaction energies on the order of -1.0 kcal/mol. Although there appears to be a slight inverse correlation between $\Delta\Delta G_{inter}$ and distance, this relationship is probably not significant considering the measured experimental errors. However, it is clear that the interaction energy vanishes when two aromatic side chains are separated by greater than ~ 7 Å from each other as is the case for Tyr55–Trp57 and Phe123–Tyr141.

The combined results of Figure 4b form a thermodynamic triple mutant cycle that probes all side-chain interactions in the Phe123–Trp143–Tyr141 triad. This analysis evaluates not only pairwise interaction energies but also potential cooperative effects between all three residues.²⁷ To this end, interaction energies between pairs of residues in the presence (left column) and absence (right column) of the third residues in the triad are compared. The results show that the pairwise interaction energies are stronger with the third aromatic side chain present than in its absence. For example, the interaction energy between Phe123 and Trp143 is -1.3 ± 0.4 kcal/mol in the presence, but -0.9 ± 0.2 kcal/mol in the absence of Tyr141. Although given the experimental uncertainties, the difference is marginal; the same trends are observed for all three pairs in the triad. Therefore, we believe that there may be some evidence for weak cooperative interactions in this group of stacked aromatic residues.

Thermodynamic Interfacial Hydrophobicities of Aromatic Residues of OmpA and Comparison to Existing Thermodynamic Hydrophobicity Scales. Next, we were interested how the measured hydrophobicities of the aromatic residues of OmpA compared with predictions from thermodynamic hydrophobicity scales. To obtain values of the thermodynamic contributions of isolated aromatic residues, we need to subtract contributions from nearest aromatic neighbors, where they exist. For example, the contribution of the isolated Trp7 residue to the thermodynamic stability of OmpA is obtained by subtracting $\Delta\Delta G_{inter}(Trp7-Tyr43)$ from $-\Delta\Delta G_u^0$ of W7A, which is equivalent to subtracting $-\Delta G_{u,H_2O}^0$ of W7A/Y43A from $-\Delta G_{u,H_2O}^0$ of Y43A. To keep sign conventions with energies of unfolding (rather than folding), which is the common convention in hydrophobicity scales, we just need to switch the signs of the four free energies listed in the previous sentence. We thus obtain a free energy contribution of 2.6 kcal/mol for the isolated Trp7. This and the free energy contributions of the other isolated aromatic residues that were obtained by this procedure are listed in Table 3. The analysis shows that single isolated tryptophanes contribute on average -2.0 ± 0.4 (standard error of the mean) kcal/mol to the stability of OmpA. The average contribution of single isolated tyrosines is -2.6 ± 0.3 kcal/mol. By comparison, single isolated phenylalanines contribute on average only -1.0 ± 0.2 kcal/mol to the stability of OmpA. Tyr168 has been excluded from these averages for reasons detailed above. Disregarding this outlier, the consistent results of the three types of aromatic residues according to this analysis are quite remarkable. It is also remarkable that the

Table 3. Distances from Membrane Center and Contributions to the Thermodynamic Stability of Individual Aromatic Side Chains Relative to Alanine

	$\Delta G_{u,H_2O}^0$ subtractions	distance from membrane center (Å)	$\Delta\Delta G_u^0$ kcal/mol
Trp7	Y43A – W7A/Y43A	7.6	2.6
Trp15	WT – W15A	11.5	2.1
Trp57	WT – W57A	12.3	2.0
	Y55A – Y55A/W57A		1.7
Trp143	F123A/Y141A – F123A/Y141A/W143A	7.1	1.6
Tyr43	W7A – W7A/Y43A	9.4	2.8
Tyr55	WT – Y55A	9.8	2.5
	W57A – Y55A/W57A		2.2
Tyr129	WT – Y129A	6.9	2.7
Tyr141	W143A – Y141A/W143A	7.9	2.6
	F123A/W143A – F123A/W143A/Y141A		3.0
Tyr168	F170A – Y168A/F170A	10.2	-1.2
Phe51	WT – F51A	4.5	1.3
Phe123	W143A – F123A/W143A	7.1	0.7
	F123A/W143A – F123A/Y141A/W143A		1.1
Phe170	Y168A – Y168A/F170A	8.8	1.0

Table 4. Comparison of Aromatic Contributions to the Stability of OmpA with Experimentally Derived Hydrophobicity Values of Aromatic Side Chains Relative to Alanine

	$\Delta\Delta G_{Trp-Ala}$	$\Delta\Delta G_{Tyr-Ala}$	$\Delta\Delta G_{Phe-Ala}$
OmpA (this work)	2.0	2.6	1.0
WW-interface ¹¹	2.0	1.1	1.3
WW-octanol ¹²	2.6	1.2	2.2
HvH-interface ^a	0.6	0.6	0.4
HvH-center ¹⁵	-0.2	-0.6	0.4

^a Extrapolated from a combination of Figures 2 and 3 of Hessa et al.¹⁵

results for the Trp and Phe agree very well with predictions from interfacial hydrophobicity scales as will be discussed in more detail in the next section. Finally, it is interesting to note that the recorded energies do not appear to depend on the depth of these residues in the membrane in the limited range that was probed with the natural positions of aromatic side chains in OmpA (Table 3 and Figure 3b).

Discussion

It has long been recognized that aromatic residues are highly enriched in the regions of membrane proteins that contact the lipid bilayer–water interface.^{1–3,8–10} This enrichment is rationalized by a significant contribution of these residues to the folding and stability of membrane proteins, mainly through their relatively high energies of partitioning to the membrane interface.¹¹ The results of the present work confirm for the first time for a real membrane protein with a defined tertiary structure that aromatic residues indeed stabilize membrane proteins as had been suspected on the basis of the earlier partition experiments and bioinformatic approaches. Not only is this general concept experimentally confirmed, but the earlier estimates of aromatic side-chain partitioning have also proven to be quantitatively largely correct. The most straightforward procedure is to compare the effect of our aromatic replacements in OmpA with the enhancement of aromatic over alanine partitioning on the Wimley–White (WW) interface scale (Table 4). The free energy values for Trp and Phe are almost the same in the OmpA folding and peptide partition systems. However, the Tyr replacement has a much larger effect on OmpA folding

than on peptide partitioning. In fact, Tyr stabilizes OmpA more than Trp, whereas Tyr containing model peptides partition less favorably to the interface than Trp containing peptides. The reason for this discrepancy is unknown, but we speculate it might be due to the higher amphiphilicity of Tyr, which may provide a stronger interfacial anchor for an integral membrane protein with defined structure than for a small peptide, which may have more degrees of freedom in the interface. It has also been shown that Tyr is more oriented (“snorkeling effect”) within the interface than Trp in membrane proteins.⁴ Interestingly, Tyr is the most over-represented aromatic side chain in the interface of membrane proteins of known structure.^{4,8} The second most over-represented residue is Trp, and Phe is third. The Hessa–von Heijne (HvH) biological interface scale (which we extrapolated here from the data given in their paper) shows smaller absolute free energy values but the same general trends (orders of side chains) that we observe in the OmpA folding studies. Trp and Tyr have slightly higher values than Phe as judged by both experiments. As Hessa et al. note, their values are “apparent” ΔG 's based on biological experiments and therefore, a scaling factor can be expected to exist between the two sets of values. The WW-octanol and HvH-center scales are probably less relevant for this comparison because the aromatic side chains are located in the membrane interface-contacting region of OmpA.

Free energies of partitioning have also been estimated from the statistics of the occurrence of amino acids at various depths in the lipid bilayer.^{5–7} These energies were on the order of 0.5 to 0.9 kcal/mol for Trp and Phe and 0.3 to 0.5 kcal/mol for Tyr. The statistical analyses make numerous assumptions that are not so easy to compare directly with experimental results. If we simply look for rank order, evolution seems to have followed thermodynamics for Trp and Phe, but not for Tyr, which contributes more to the stability of at least OmpA than would be guessed from the statistical analyses.

An interesting and important result of this study is that aromatic side chains interact with each other if they are within a range of 6 or perhaps 7 Å. Aromatic–aromatic side chain interactions apparently play a significant stabilizing role in the folding of OmpA. Some of these interactions occur within individual β -strands, but more frequently they are found between side chains on adjacent β -strands. Whether interstrand or intrastrand, these interaction energies are on the order of -1 kcal/mol (Table 2). Our values are in excellent agreement with previously determined interaction energies between aromatic side chains in soluble proteins and model peptides, which are in the -0.3 to -1.3 kcal/mol range,^{37–40} that is, similar in magnitude to weak salt bridges and standard hydrogen bonds between side chains. There appears to be no dependence of the interaction energies on context, that is, whether the residues are adjacent in sequence or diagonal across strands, but the

number of data points is probably too small to reach a definite conclusion on this issue.

To gain more insight into how frequent and important interaromatic side-chain interactions might be in membrane proteins, we surveyed pairs of aromatic side chains within 7 Å of each other in six nonhomologous membrane proteins of known structure. The survey includes three α -helical (bacteriorhodopsin, the potassium channel KcsA, and lactose permease) and three β -barrel (OmpA, OmpF, and BtuB) membrane proteins (see Supporting Information table). In these six proteins, between 7% and 18% of all residues that face the lipid bilayer are aromatic residues. Remarkably, 50 to 70% of these aromatic residues have the potential for aromatic–aromatic stacking interactions with intercentroid distances of less than 7 Å. Similarly, Burley and Petsko found that approximately 60% of all aromatic side chains are within 7 Å range of each other in soluble proteins.¹⁹ The larger membrane proteins tend to have more such pairs than the smaller ones. BtuB has 18 and lactose permease has as many as 64 potential sites for aromatic side-chain interactions. Potential inter- and intrastrand aromatic interactions are approximately equally frequent in helical and β -sheet membrane proteins except for lactose permease and BtuB where the proportion of interstrand aromatic pairs is higher. It is also interesting that the proportion of lipid-facing and protein-facing aromatic residues that are involved in aromatic–aromatic interaction are quite different in α -helical and β -barrel membrane proteins (Supporting Information table). In β -barrel membrane proteins, most clustered aromatic side-chains are lipid-facing, but in α -helical membrane proteins, most clustered aromatic side chains are protein-facing and thus contribute to helix packing in these proteins. Some aromatic stacking interactions could potentially also contribute to inter-subunit interactions in oligomeric membrane proteins. For example, eight inter-subunit aromatic pairs per monomer are found in the OmpF trimer and four inter-subunit aromatic pairs per monomer are found in KcsA. This analysis strongly suggests that aromatic residues stabilize membrane proteins not only individually through their interaction with the membrane-water interface, but also collectively through clustering in this chemically distinct membrane compartment. In conclusion, this work shows that tyrosines are particularly powerful in anchoring membrane proteins in the membrane interface and that aromatic clustering in the interface can provide a substantial driving force for the folding and oligomerization of integral membrane proteins.

Acknowledgment. This work was supported by a grant from the NIH (Grant GM051329).

Supporting Information Available: A supporting table describing the structural analysis of aromatic clustering in six nonhomologous membrane proteins. This material is available free of charge via the Internet at <http://pubs.acs.org>.

(37) Serrano, L.; Bycroft, M.; Fersht, A. R. *J. Mol. Biol.* **1991**, *218*, 465–75.

(38) Smith, C. K.; Regan, L. *Science* **1995**, *270*, 980–2.

(39) Tatko, C. D.; Waters, M. L. *J. Am. Chem. Soc.* **2002**, *124*, 9372–3.

(40) Mahalakshmi, R.; Raghothama, S.; Balaram, P. *J. Am. Chem. Soc.* **2006**, *128*, 1125–38.